

C-1

150



Measurement of the Radiative Properties of Air at High Temperatures and Pressures

E. A. Larson, R. T. Murray, et al.

School of Mechanical Engineering
Georgia Institute of Technology
Atlanta, Georgia 30332

October 1979

Final Report for Period June 1977 — May 1979

Approved for public release; distribution unlimited.

Property of U. S. Air Force
AEDC LIBRARY
F40600-77-C-0003

AEDC TECHNICAL LIBRARY



5 0720 00036 6312

**ARNOLD ENGINEERING DEVELOPMENT CENTER
ARNOLD AIR FORCE STATION, TENNESSEE
AIR FORCE SYSTEMS COMMAND
UNITED STATES AIR FORCE**

NOTICES

When U. S. Government drawings, specifications, or other data are used for any purpose other than a definitely related Government procurement operation, the Government thereby incurs no responsibility nor any obligation whatsoever, and the fact that the Government may have formulated, furnished, or in any way supplied the said drawings, specifications, or other data, is not to be regarded by implication or otherwise, or in any manner licensing the holder or any other person or corporation, or conveying any rights or permission to manufacture, use, or sell any patented invention that may in any way be related thereto.

Qualified users may obtain copies of this report from the Defense Documentation Center.

References to named commercial products in this report are not to be considered in any sense as an indorsement of the product by the United States Air Force or the Government.

This final report was submitted by Georgia Institute of Technology, Atlanta, Georgia 30332, under contract F40600-77-C-0007, with the Arnold Engineering Development Center/DOT, Arnold Air Force Station, Tennessee 37389. Mr. Marshall K. Kingery, Directorate of Technology, was the AEDC project manager.

This report has been reviewed by the Information Office (OI) and is releasable to the National Technical Information Service (NTIS). At NTIS, it will be available to the general public, including foreign nations.

APPROVAL STATEMENT

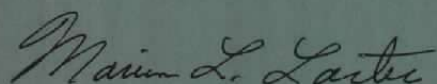
This report has been reviewed and approved.



MARSHALL K. KINGERY
Project Manager
Directorate of Technology

Approved for publication:

FOR THE COMMANDER



MARION L. LASTER
Director of Technology
Deputy for Operations

UNCLASSIFIED

DD FORM 1 JAN 73 1473 EDITION OF 1 NOV 65 IS OBSOLETE

UNCLASSIFIED

UNCLASSIFIED

20. ABSTRACT (Continued)

excellent agreement. Laser transmission experiments at 632.8 nm show that ray refraction in the arc and its boundaries warrants attention at 30 atm in experiments in which intensities are being measured. A number of observations relating to work at still higher pressures were made.

UNCLASSIFIED

PREFACE

The research reported herein was conducted by the Georgia Institute of Technology, School of Mechanical Engineering, Atlanta, Georgia for the Arnold Engineering Development Center (AEDC), Air Force Systems Command. The report covers work from June 1977 through May 1979 under Contract F40600-77-C-0007. The Air Force project manager for this contract was Marshall K. Kingery, Directorate of Technology, AEDC, Arnold Air Force Station, Tennessee.

CONTENTS

	<u>Page</u>
Introduction.	7
Original Apparatus.	9
Preliminary Experiments	12
Argon Arc.	12
Air Arc.	12
Summary.	16
Apparatus Modification I.	16
Air Arc Experiments on Absorption	19
Improvements	19
Temperature Profiles Corrected for Absorption.	19
Argon Arc Experiments on Refraction, I.	24
Extended Backlight	24
Laser Backlight.	27
Apparatus Modification II	28
Argon Arc Experiments on Refraction, II	34
Theoretical Refraction Estimates.	34
Discussion	37
Conclusions.	39
References	40

LIST OF FIGURES

Figure		Page
1.	Schematic of Experiment.	10
2.	Cascade Arc.	11
3.	Schematic of Arc Region and Transmission Measurement Setup.	13
4.	Relative Transmission, Argon Arc, $\lambda = 546.4$ nm	14
5.	New Plates	17
6.	Apparatus Modification, I.	18
7.	First Approximation for Radial Temperature Profiles. Arc Assumed Optically Thin	20
8.	Comparison of First Temperature Approximation with Final Temperature Profile Using the Oxygen 844.65 nm Spectral Line Data	20
9.	Comparison of First Temperature Approximation with Final Temperature Profile Using the Nitrogen 862.92 nm Spectral Line Data.	22
10.	Final Temperature Profiles from Data for the Two Spectral Lines	22
11.	Effect of Arc Absorption Upon the Predicted Intensity Profiles Using the Final Radial Temperature Profiles for the Two Spectral Lines. Air Arc, 30 Atm., 11.9 amp.	23
12.	Horizontal Scan at Different Vertical Positions, Backlight Only. $\lambda = 842.35$ nm, Argon Arc, 30 Atm., = 15 amp	25
13.	Horizontal Scan at Different Vertical Positions. Arc Only. $\lambda = 842.35$ nm, Argon Arc, 30 Atm., = 15 amp.	25
14.	Midplane Scans From Figures 12 and 13 Superimposed, Vertical Scales Differ	26
15.	Scaled Relationships of the Scan in Figure 12 to the Apparatus.	29
16.	Layout of Preliminary Beam Refraction Experiment	30
17.	Results of Preliminary Beam Refraction Experiment.	31
18.	Apparatus Modification, II	32

LIST OF FIGURES (Continued)

Figure		page
19.	Window Detail of Figure 18. Top View.	33
20.	Mask Detail of Figure 19. End View.	33
21.	Sketch of Effect of Refraction on Laser Beam Shape	35
22.	Geometry for Estimating the Angle of Deviation	35

INTRODUCTION

The Arnold Engineering Development Center has research programs in which the design of high power arc heated wind tunnels calls for knowledge of the properties of air near 10,000°K and 250 atm. There is no experimental information for those conditions. The theoretical predictions come from a semiempirical theory in which the more poorly-known collision probabilities are empirically "tuned" to obtain agreement with experimental data at 1 atm. Errors may arise in the extrapolation of the results to 250 atm, because the change in air composition causes a change in the relative importance of the different types of collisions. Thus, experimental information that could be obtained at higher pressures would be valuable in "tuning" the semi-empirical theories up to the pressures of interest.

AEDC has been supporting an experimental program at Georgia Tech to measure the electrical and thermal conductivities and the total radiation of air at high temperatures and pressures (Ref. 1). The test plasma is produced in a wall-stabilized arc which is viewed transversely. Spectroscopic techniques are used to determine the temperature profile in the arc and spectral and total radiation measurements are made. The central problem is to relate the various detector outputs to the local conditions in a plasma volume element in order to determine the element temperature and to obtain the radiation characteristics of air at that temperature and pressure. The latter is of direct engineering interest but also must be known if the thermal conductivity is to be deduced from the power balance equation for the test plasma.

In the arc apparatus, the drop of pressure and temperature to the laboratory environment is unavoidable. The light rays emanating from within the arc are subject to refraction as they pass through the strong gradients. The rays are also subject to partial reflection from surfaces and to absorption and scattering in the arc and in the media between the arc and the detectors. All of the above phenomena can cause a change of signal. In addition, refraction can obscure the solid angle relationships between the arc and the detector elements as well as the exact location of the source element. Reflection and scattering also obscure the source element location and intensity.

The phenomena do not cause serious difficulties at lower arc pressures but warrant attention as the pressures reach and exceed 30 atm.

The earlier work (Ref. 1) was done at pressures of 1, 6, and 30 atm with arc centerline temperatures near 10,000°K. At the start, because of the status of the knowledge of air properties, the technology of air arcs, and reservations about the applicability of certain spectroscopic techniques, it was decided to begin the experiments at 1 atm. and to increase the pressure through the largest practical steps.

The arc technology was extended successfully so that a central pure-air section of the arc column could be established while shielding the electrodes with argon to minimize electrode damage. The work produced measured electrical conductivity values for air which are in good agreement with other experiments at 1 atm. and with theoretical predictions at 1 and 6 atm. The agreement with theory at 30 atm. is fair. The total

radiation measurements were not so complete, and could be expressed only in terms of lower limits on the radiation. Consequently, the deduced values of thermal conductivity represent only upper limits. Nevertheless, the thermal conductivity does agree well with measurements at other laboratories at 1 atm., and with the theoretical predictions at 1 and 6 atm. Again, at 30 atm. a discrepancy between theory and experiment appears. The good agreement for thermal conductivities at the lower pressures is probably attained because radiation is not a major term in the power balance.

As the research was extended beyond 30 atm. to 100 atm. (Ref. 1) it became clear that a major loss of radiation occurred between the arc and the detectors due to the intervening medium. The radiation loss must be dealt with, so the emphasis of the program shifted to that problem.

The work to be reported here deals with the identification of the cause of absorption outside the arc, improvements in apparatus design to reduce the absorption, corrections for that absorption and for self-absorption within the arc and finally, an assessment of the refraction problem. Most of the experiments were done at 30 atm.

ORIGINAL APPARATUS

The experimental set-up used in the previous contract (Ref. 1) is shown in Figure 1. The arc is located in the center (region I) of a pressure vessel about 10 inches in diameter. A spectrometer views the arc via the quartz window(s), a front-surfaced mirror, and a lens. The details of the cascade arc are seen in Figure 2. The arc radius is 1.5 mm., the inner quartz window separating regions II and III is about 1 inch from the arc axis, and the outer window separating regions III and IV is about 6 inches off axis. The outer window supports the pressure drop.

In operation, the total vessel is purged with argon at 1 atm. before the arc is struck. The vessel is then capped and charged to high pressure. Then the air flow is started and the flows are adjusted until a pure air arc is obtained in region I. When the arc in region I is pure air, the high pressure gas mixture composition differs in regions II and III on either side of the inner quartz window. The initial transmission experiments indicated that most of the signal loss at 100 atm. occurs in the inner regions I and II.

The copper cascade plates are cooled by internal water flows which come within 1.5 mm. of the channel wall. Thus, the large temperature gradients in the experiment occur quite near the arc whereas the pressure drop occurs across the outer window between regions III and IV. Refraction is most likely to occur therefore near the arc, and possibly across the inner quartz window if the change in composition of the gas mixture across the window is significant.

In Figure 2, it is seen that between regions I and II, the copper plates slope away to enlarge the plate separation which is perpendicular to the optical path. The plate surfaces here are blackened electrochemically to minimize reflections. The inner quartz windows are tilted about 50° off vertical so that reflections from their surfaces do not enter the detectors. Reflections from the surfaces of the outer windows are accounted for by the method of images and are located by means of an auxiliary laser. In Figures 1 and 2, if region I is backlighted along ray C and viewed along direction B, one sees a rectangular region which is approximately .3 mm high and 10 mm wide. Region I is imaged in focus on the spectrometer slits with a magnification of 2.7. The spectrometer slits are set typically at .2 mm. high (on image center) and .03 mm. wide (at any lateral position). These settings further reduce the problem of reflections in the arc apparatus near the arc.

Early in the present contract period, the inner quartz windows were removed. A backlighting assembly was added at "C" and another recording channel was added to the output of the picoammeter. The assembly consisted of a source, chopping wheel and shutter. The second recording channel consisted of a lock-in amplifier followed by a strip chart recorder. With the new equipment, transmission and/or emission studies can be conducted.

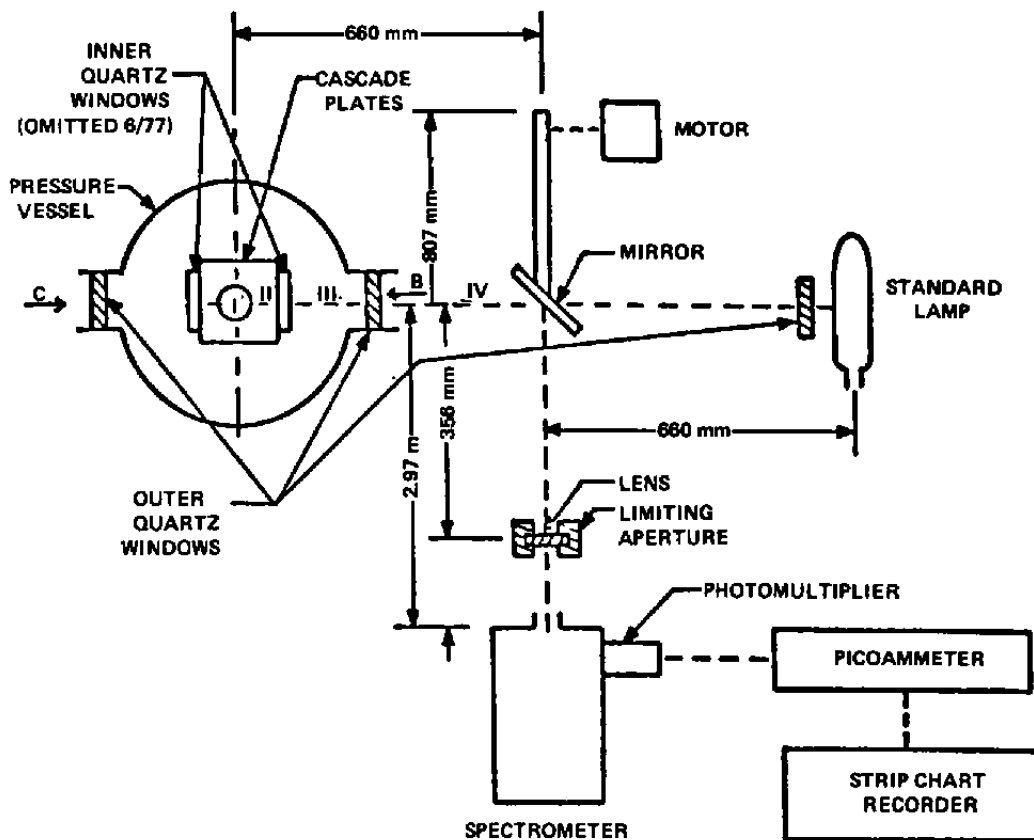


Figure 1. Schematic of Experiment.

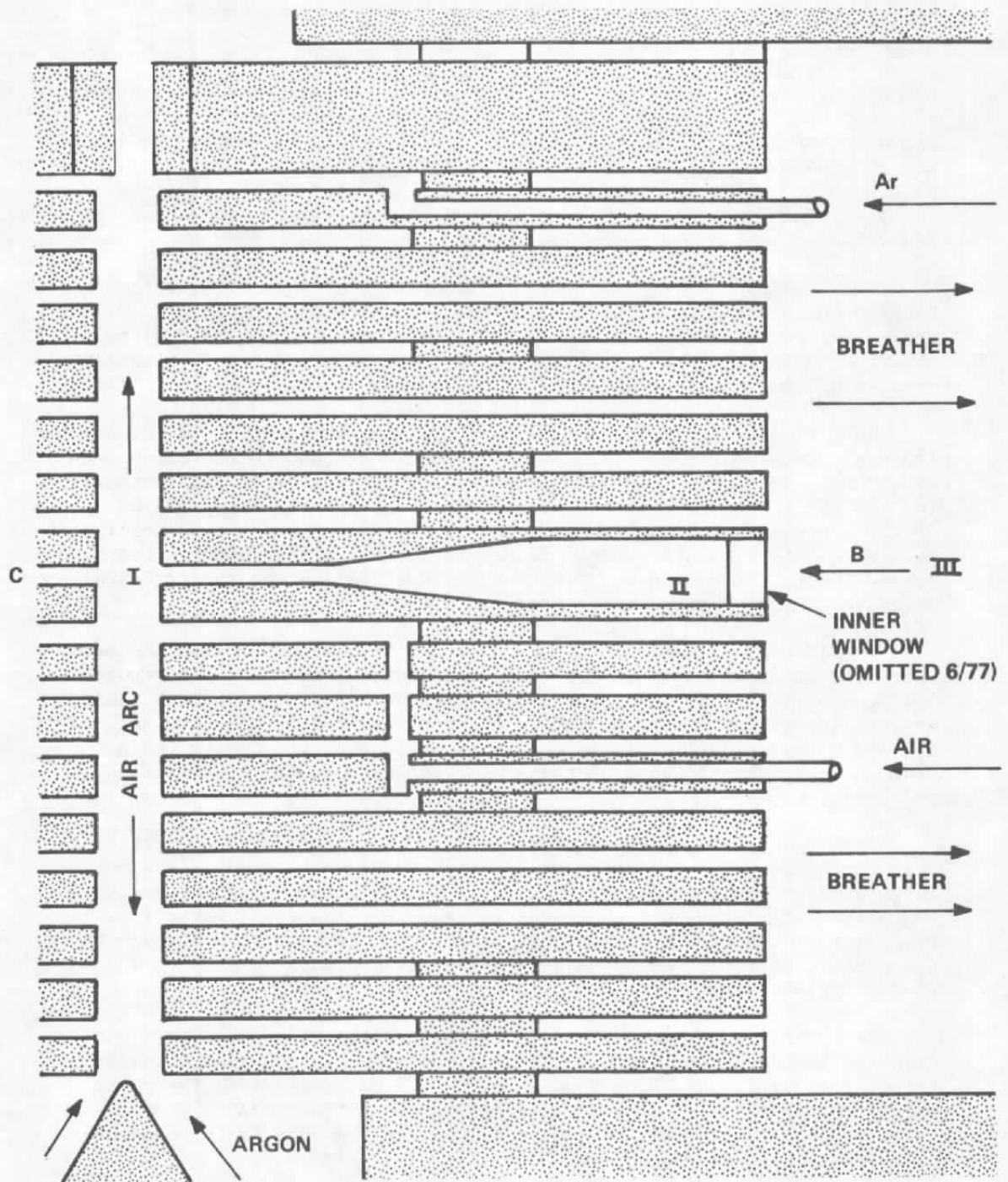


Figure 2. Cascade Arc.

PRELIMINARY EXPERIMENTS (Ref. 2)

ARGON ARC

As discussed in the introduction, previous experiments had indicated a strong loss in signal for the air arc at pressures above 30 atm. in regions I and II of Figures 1 and 2. It was decided to remove the inner quartz windows in an attempt to reduce the air by-products in region II. Although that might introduce complications in eventual data analysis due to additional flow effects, the goal at that time was to concentrate on reduction of the signal loss.

The initial experiments (Ref. 2) were aimed at establishing the background information necessary for the transmission experiments. The set-up of Figure 1 is abbreviated schematically in Figure 3(a) to show the essential features of the measurement of the lateral intensity profile of the transmitted light.

The initial backlight source was a 100 w Hg arc lamp. The intense lines at 364.9 nm., 546.1 nm., and 815.5 nm. were used to represent the spectrum of interest. The apparatus was filled with argon and pressurized. The arc was not struck. The lateral transmission intensity profiles of the above lines through the argon at room temperature showed negligible changes as the pressure changed from 1 to 100 atm. This observation also served to calibrate transmission changes (negligible) due to structural stresses in the pressure vessel and its windows.

The lateral transmission scans on argon were repeated with the arc operating at about 15 amp. Typical scans (Ref. 2) are shown in Figure 4. The scan at 1 atm. was the same whether or not the arc was on and thus serves also as the baseline data (cold-argon) at 30 atm. The presence of the arc causes a small loss in transmission through its center and a drastic loss near the edge of the arc. Farther out, the transmission recovers.

The signal loss has been attributed (Ref. 2) to a strong refraction zone surrounding the arc as shown in Figure 3(a). The zone is due to a large gradient in the refractive index. The deviation of a ray varies as the sine of the angle between the ray and the gradient. Thus it follows that the effect would be small for light transmitted through the arc center, in the midplane between the cascade plates which form the window region.

In further experiments, it was found that the major loss in signal in Figure 4 occurred over the water channels in the plates, said channels being at least 1.5 mm. from the arc bore (1.5 mm. radius) in the plate. The effect is pressure dependent. The loss is not noticeable up to about 6-7 atm., but the valleys in Figure 4 appear and deepen as the pressure is further increased.

AIR ARC

After the argon data was taken, air was injected into the test channel, at first in small amounts, then in sufficient quantity to achieve air purity

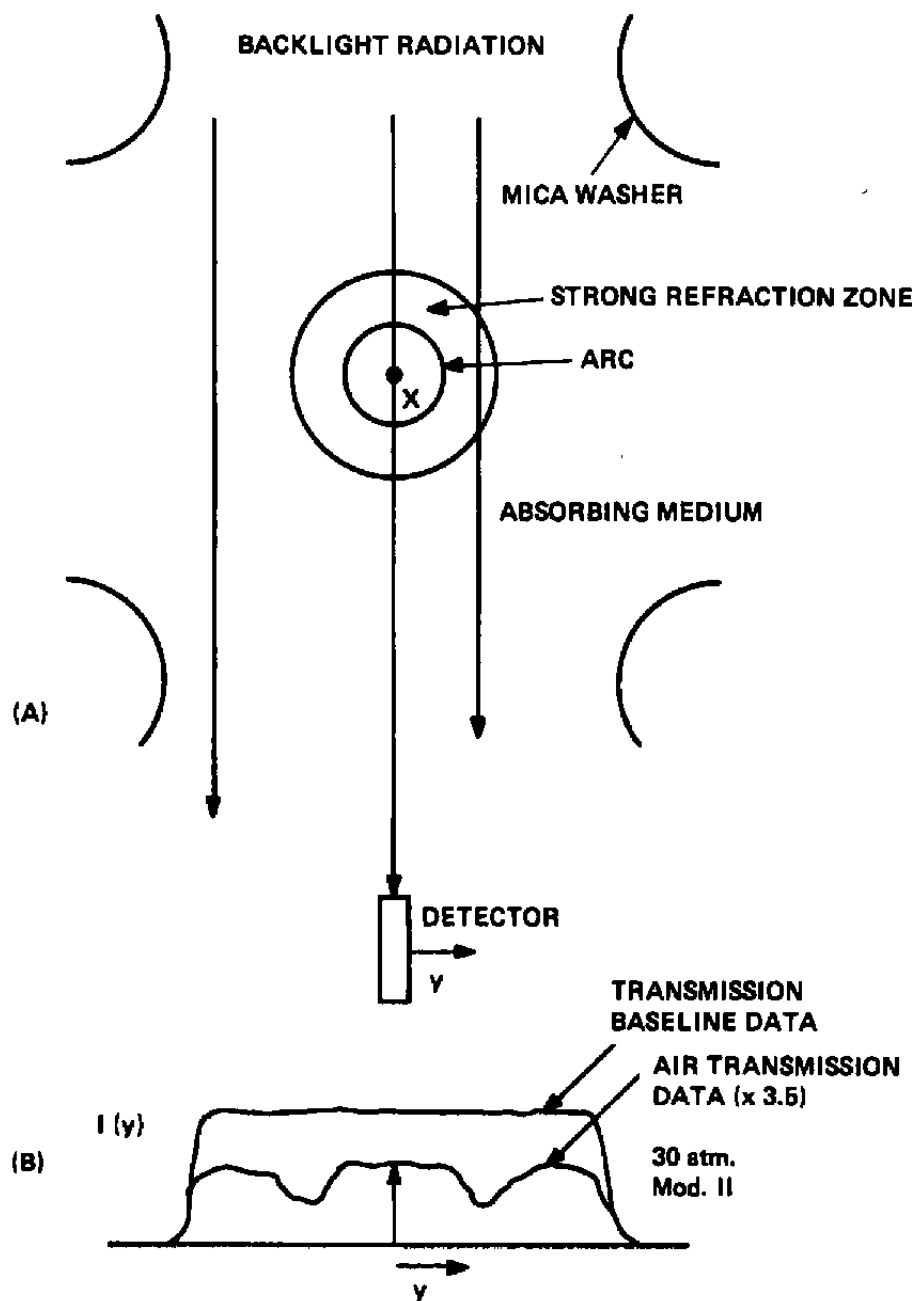


Figure 3. Schematic of Arc Region and Transmission Measurement Setup.

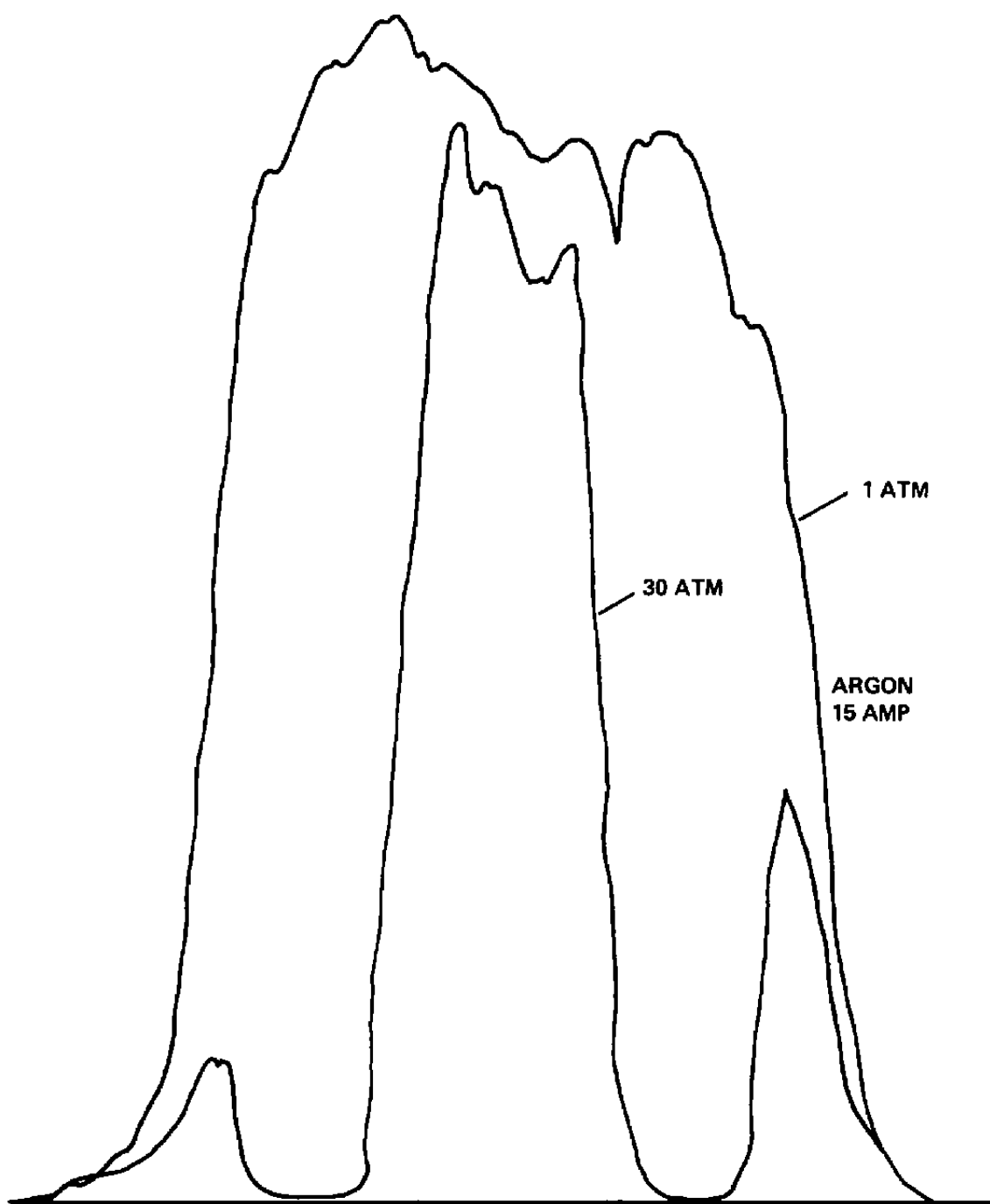


Figure 4. Relative Transmission, Argon Arc
 $\lambda = 546.4 \text{ nm}$

in the test section. The 30 atm. argon curve in Figure 4 serves as the baseline for the air experiments at 30 atm. It was observed (Ref. 2) that at the first indication of air, the central plateau began to drop, but the other features remained approximately the same. When air purity was achieved, the intensity through the arc center at $\lambda = 546.4$ nm. had dropped at least $\times 100$ and perhaps as much as $\times 200$. (The rejection ratio of the lock-in amplifier was 200, so the accuracy was poor.)

Work was done to identify the cause of the additional losses due to the presence of the air. Spectral measurements showed that the test channel could be switched from argon to air or vice versa in less than one minute. If the channel had run on air for several minutes, however, it would take region II in Figure 2 (no inner window) several minutes more to recover to argon than the arc channel in region I. Thus an absorption spectrum could be run on the medium in region II. This was done and the absorption spectrum (Ref. 2) was identical to that of NO_2 . No further work was done to characterize the medium, but it is clear that the major loss is due to NO_2 in the region between the arc and the outside edge of the window plates.

It is fortunate that the NO_2 absorption spectrum peaks near 400 nm. since the only lines available for temperature measurements at 30 atm. are at wavelengths above 700 nm (Ref. 2). Since the confidence one can establish in the measured temperature profile is of prime importance, the effort shifted to the higher wavelengths.

The backlight was changed to a 1000 W Xe arc lamp to obtain a better ratio between the chopped backlight intensity and the steady arc intensity in the 800 nm. to 900 nm. wavelength range. The Xe 834.4 nm. line was used for an intense source, and the continuum at 844.7 nm. was also used since the oxygen line at that wavelength is an important emission line in the arc.

The question arose, given a continuous NO_2 production, whether or not the environment would change so quickly over a set of experiments as to prohibit suitable accuracy in the radiation experiments which depend upon the calibration of the environment at a point in time. To answer the question, the argon arc was established at 30 atm. and the test section was quickly changed to pure air in less than a minute. The emission from the arc and the transmission through the center of the vessel were monitored continuously before and after the air injection was started. The arc emission stabilized within a minute of achieving air purity and did not deteriorate for the tracking interval of 24 min. The transmission took a sharp drop, but then slowly changed from a drop of $\times 10$ four minutes after air injection to a drop of $\times 13$ ten minutes after air injection. The wavelength being observed was 834.4 nm. At the center of the 844.7 nm. oxygen line, the drop appeared to be perhaps $\times 2$ greater. Since the property measurements of interest only require a minute each, it appears that the environment calibration changes are slow enough not to prohibit this particular cascade from being useful in temperature and electrical conductivity measurements.

SUMMARY

In the apparatus of Figure 2 without the inner window, the channel can be switched from argon to air in less than a minute at 30 atm. By-products fill up the region II over the next three or four minutes but reach a nearly steady distribution as shown by the arc emission and the backlight transmission experiments. The transmission drop across the entire vessel is about X13 for a wavelength of 834.4 nm. which implies the square root of that for the transmission drop from the arc center to the vessel outer window. The transmission drop does not depend strongly upon which part of the arc is transversed which implies that the arc is nearly optically thin and that the medium surrounding the arc is the cause of the absorption losses. The absorption has been identified (Ref. 2) as mostly due to NO_2 .

At the edge of the arc there is an additional strong loss of signal due to ray-bending by the gradients of the index of refraction which are particularly large near the plate water channels. The ray-bending region appeared to encroach only slightly upon the edge of the arc from where emission data is taken to deduce the temperature profiles.

The apparatus could probably be used to deduce temperature profiles and electrical conductivity, but would be unsuitable for radiation measurements since the absorption by the NO_2 was too severe at the broad NO_2 absorption peak centered near 400 nm. Therefore it was decided to attempt to reduce the NO_2 concentration along the optical path.

APPARATUS MODIFICATION I

In order to reduce the concentration of NO_2 , the escape paths into the much larger vessel volume were maximized. Figure 5(a) shows the original plate construction. The only escape path was along the optical path since the rubber gasket seal prevented any other flow. In the modified apparatus, the seal was removed and the plate was cut away as much as possible without violating the water channels. See Figure 5(b). The only separators between the plates are the gaskets at the water holes. Thus the NO_2 can leave the arc region through a full 360° until the flow meets the water gaskets.

Furthermore, a comparison between Figure 6 and Figure 2 shows that several such plates are cut away so that the escaping NO_2 reaches an enlarged volume earlier than before.

In addition to the plate changes the gap between the two plates forming the window was increased four fold to 1.0 mm. This was an attempt to improve the observation of any refraction due to vertical gradients.

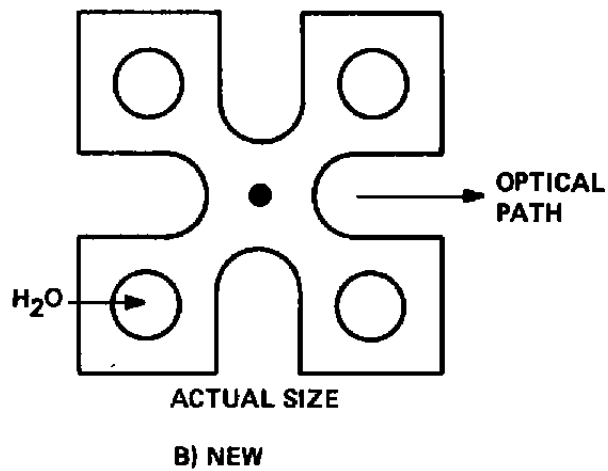
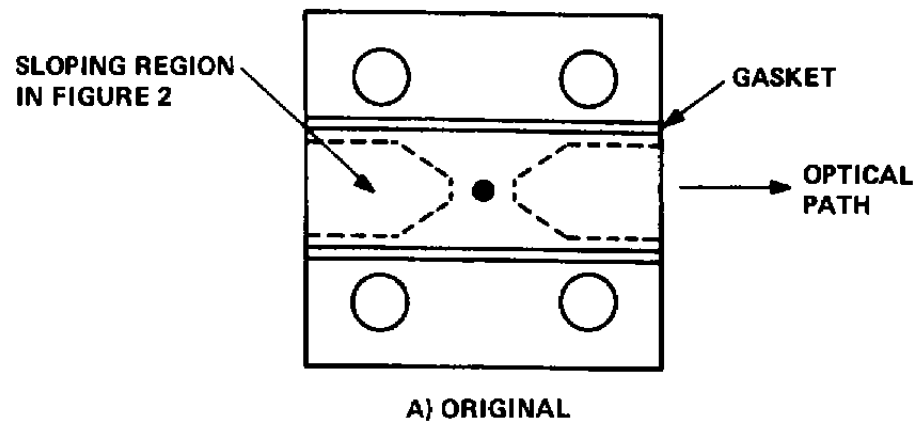


Figure 5. New Plates

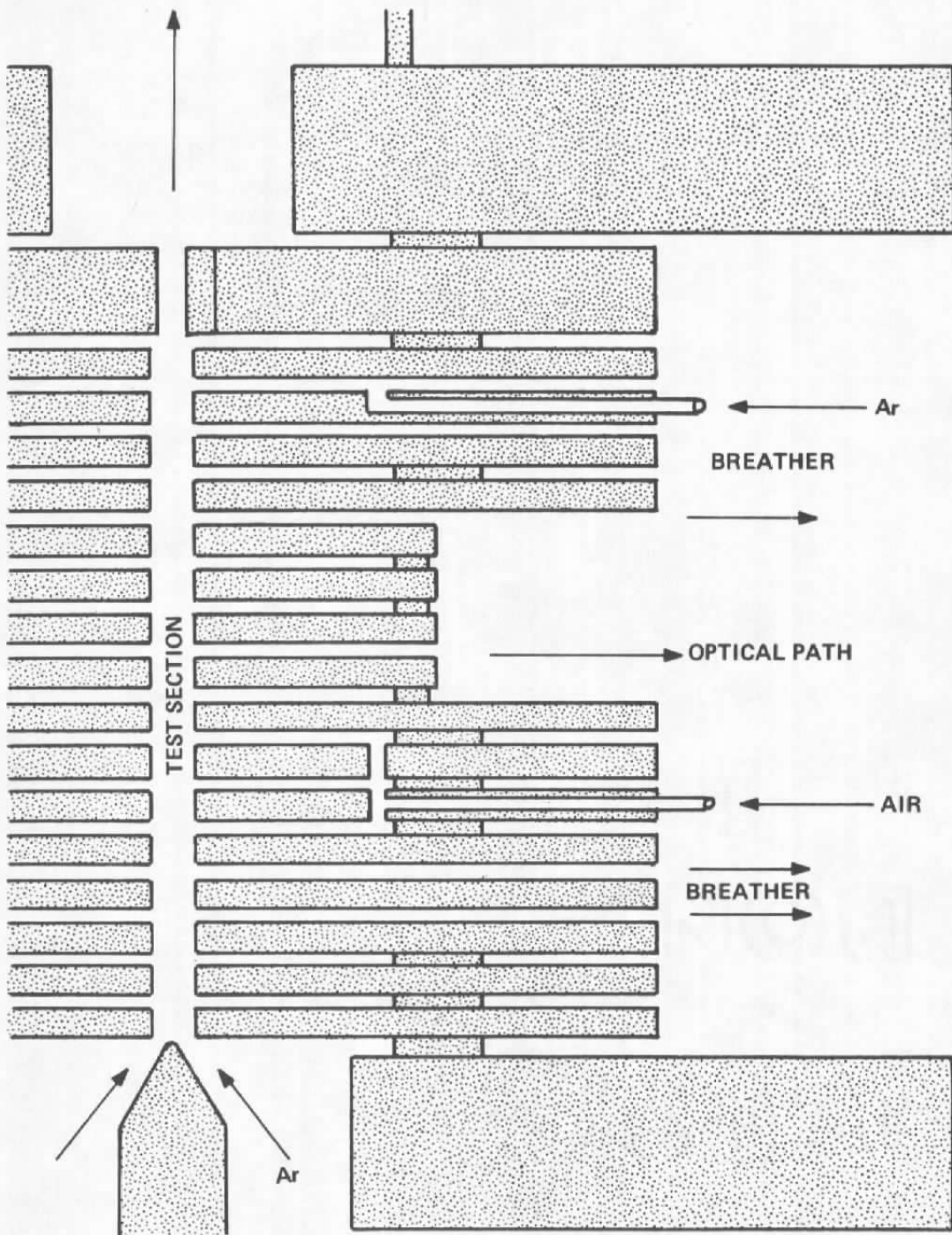


Figure 6. Apparatus Modification, I

AIR ARC EXPERIMENTS ON ABSORPTION

IMPROVEMENTS

For an air arc at 30 atm. and about 12 amp. the transmission drop through the arc center but across the entire vessel had been reduced to $X_{1.8}$ at 834.4 nm. and $X_{6.6}$ at the center of the 844.7 nm. line. The square root of those factors represent the drops from the arc center to the pressure vessel window. These factors are low enough to grant reasonable accuracy in the necessary environmental calibrations.

A major bonus of the new design was the observation that air emission spectra could be obtained across the spectrum, even near 400 nm. which had previously been impossible due to the greater amount of NO_2 . Thus one could expect to be able to obtain eventually air emission intensities corrected for the NO_2 absorption.

The other features of the preliminary experiments were found also in the new design.

TEMPERATURE PROFILES CORRECTED FOR ABSORPTION

After rechecking the results of the preliminary experiments with the new apparatus, it was assumed, that in the first iteration, the refraction effects would be ignored in the deduction of the temperature profiles.

Salmon (Ref. 3) undertook the determination of the temperature profile in an air arc operating at 30 atm. and 11.9 amp. The techniques (Refs. 4,5) used the absolute emission intensity of the OI 844.7 nm. line and the NI 862.9 nm. line corrected for self-absorption within the arc and media absorption outside the arc.

In Salmon's work, a Xe lamp was used to backlight the arc, as shown in Figure 3. In the lower sketch, the detector output is given for spatial scans with the arc off (Baseline Data) and with the arc on (Air Data). These curves are for the backlight radiation. From such curves and other information discussed previously, it was concluded that most of the drop in the backlight intensity occurred outside the arc and was due to absorption by the air by-products. The transmission along the optical path through the arc center was then used as the backlight transmission for any path through the arc region, and refraction in that region was assumed to be negligible. Assuming the arc to be optically thin as a first trial, the square root of that transmission then served as the transmission from any volume element of the arc to the detector.

With the backlight off, the arc on, spatial profiles of the line emission for the OI 844.7 nm. line and the NI 862.9 nm. line were determined and corrected for the absorption between the arc and the detector.

The corrected spatial scans were Abel-inverted to find the radial emission coefficients and from them, the temperature profiles assuming the arc to be optically thin. The results (Ref. 3) are shown in Figure 7.

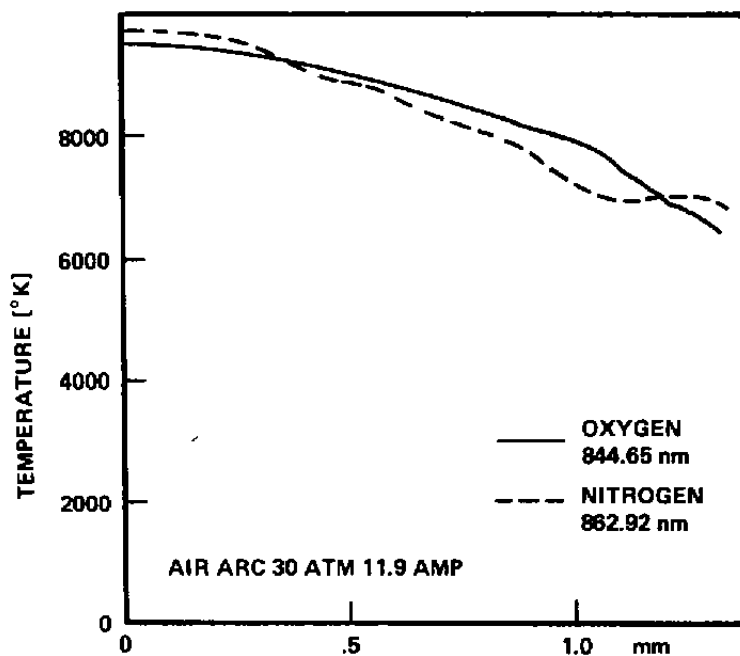


Figure 7. First Approximations for Radial Temperature Profiles. Arc Assumed Optically Thin.

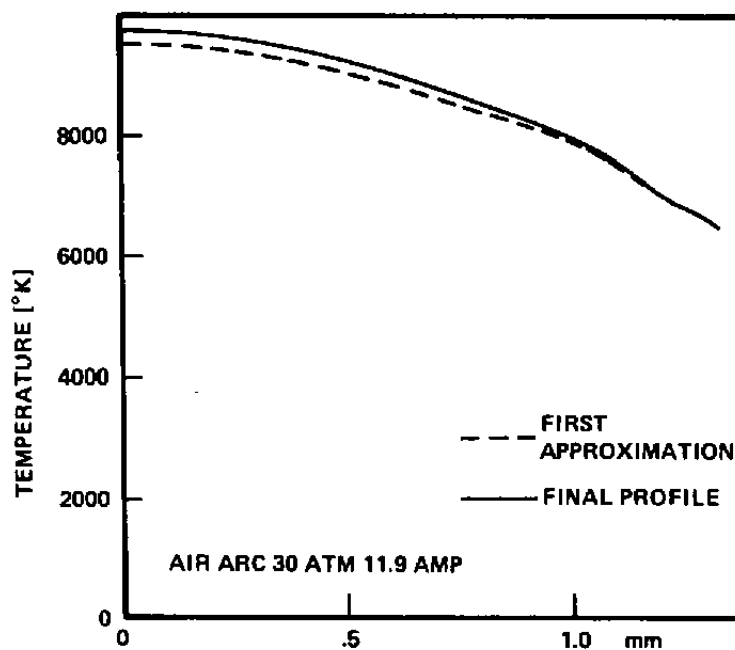


Figure 8. Comparison of First Temperature Approximation with Final Temperature Profile Using the Oxygen 844.65 nm Spectral Line Data.

Using the temperature profiles generated using the "optically-thin" assumption, the radiation transport equation

$$\frac{dI_{\lambda}}{dx} = \epsilon_{\lambda} - k_{\lambda} I_{\lambda}$$

was integrated along numerous arc chords and across each line profile within the spectrometer band-pass to generate predicted detector outputs for a spatial scan. Here I_{λ} is the spectral intensity at a linear position x along an arc chord, ϵ_{λ} is the line spectral emission coefficient, and k_{λ} is the spectral absorption coefficient.

Local thermodynamic equilibrium was assumed which allowed relating ϵ_{λ} and k_{λ} through the Planck blackbody function B_{λ}

$$\epsilon_{\lambda} = k_{\lambda} B_{\lambda}$$

In relating the line spectral coefficient ϵ_{λ} , to the total line emission coefficient ϵ_L , by

$$\epsilon_L = \int \epsilon_{\lambda} d\lambda$$

the Lorentz, Doppler, and Voigt line broadened profiles were investigated.

The temperature profiles obtained from the "optically-thin" trial were used as the first approximation in an iterative procedure which adjusted successive temperature profiles until the generated predicted detector outputs match the actual experimental intensity data to within 1%. The (Final) temperature profiles which will give a double integral (x, λ) of the transport equation matching the actual data to within 1% are compared to the "optically-thin" temperature profiles in Figure 8 and 9, and are compared to each other in Figure 10.

The temperature profiles in Figure 10 agree within experimental error. This is a major step forward in the research program since it indicates that self-absorption and the absorption in the outside medium can be corrected for in establishing the temperature profile of the air plasma.

In order to investigate the amount of self-absorption within the arc, the transport equation with $k_{\lambda} = 0$ was integrated using the final temperature profiles. The effect upon the predicted intensities is shown in Figure 11.

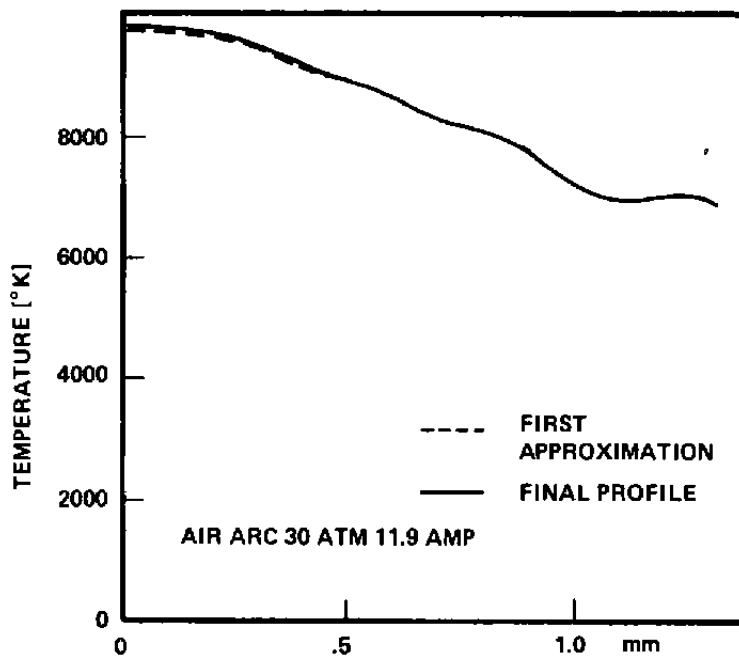


Figure 9. Comparison of First Temperature Approximation with Final Temperature Profile Using the Nitrogen 862.92 nm Spectral Line Data.

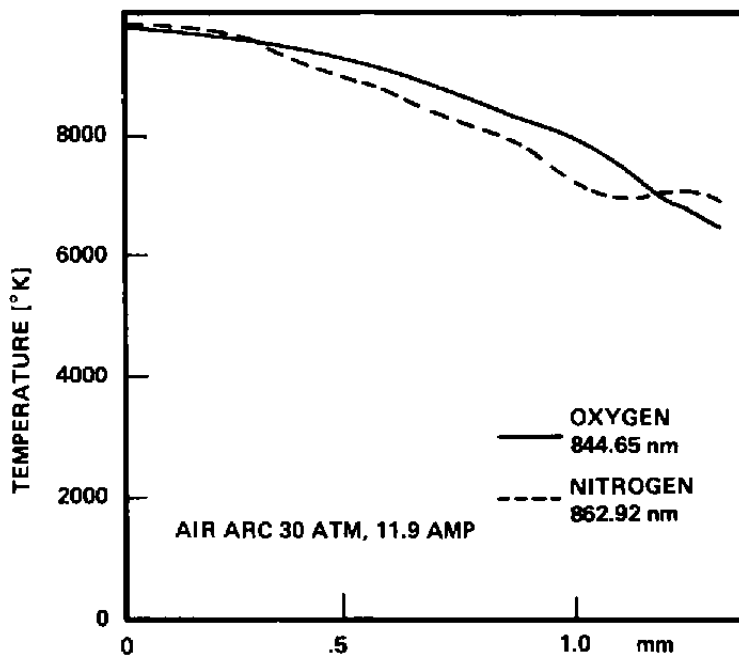


Figure 10. Final Temperature Profiles from Data for the Two Spectral Lines.

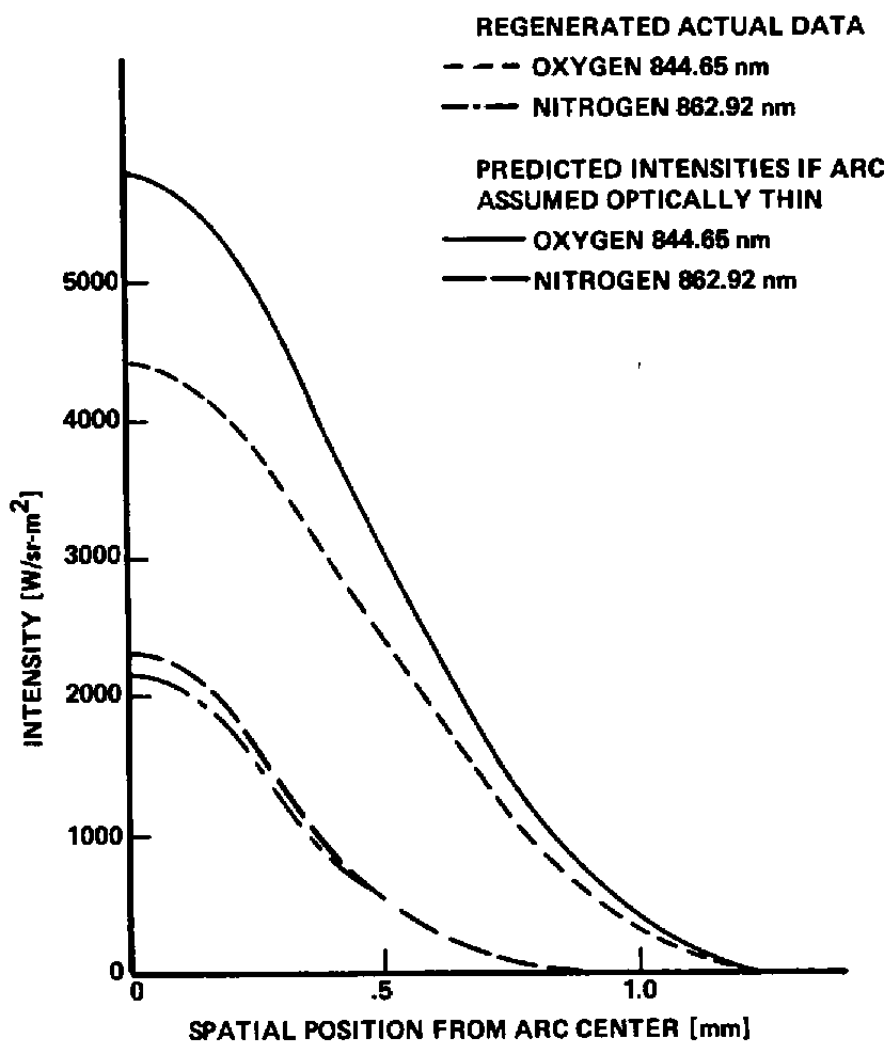


Figure 11. Effect of Arc Absorption Upon the Predicted Intensity Profiles Using the Final Radial Temperature Profiles for the Two Spectral Lines. Air Arc, 30 Atm., 11.9 amp.

Through the arc center, the predicted intensity drops from the no-absorption case to the absorption case by 24% for the oxygen line and 7% for the nitrogen line. It is expected that the oxygen line self-absorption would be larger because it has a greater emission coefficient at these pressures and temperatures.

The question naturally arises whether the oxygen line is still usable at 100 atm. A preliminary investigation indicates that it will be since the line broadens rapidly enough with pressure that the peak intensity of the line varies slowly. The self-absorption within the line across the arc central chord should still amount to about 24%.

Of course the nitrogen line will still be usable at 100 atm. since self-absorption is about 1/3 smaller.

ARGON ARC EXPERIMENTS ON REFRACTION, I

EXTENDED BACKLIGHT

The preliminary experiments on the original cascade had shown a signal loss region outside the arc due to refraction. As the arc pressure was increased, the effect became noticeable at 6-7 atm. and worsened as the pressure was increased further. The loss of signal appeared to encroach slightly upon the edge of the arc where emission data was taken for the temperature profiles. The effect was ignored in the last section in the first attempt to deduce temperature profiles with data corrected for absorption. This section describes the progress made in understanding the refraction in the new apparatus. The experiments were done on an argon arc to avoid the additional complications due to absorption.

The effect of refraction is best studied with narrow beams, but since the temperature profile studies were made with a extended backlight source, some refraction work was done with the 1000 W Xe lamp as the backlight.

Ideally, the plane in Figure 3(a) is the midplane of the plates forming the viewed cross-section as seen in Figure 6. This is tested in Figure 12 which is an overlay of the horizontal spatial scans of the image on the spectrometer for several vertical positions of the images. The signal is due to the backlight only. Figure 13 is a set of horizontal scans of the arc emission (backlight off) at different vertical positions.

The scans in Figures 12 and 13 reveal that the signals are insensitive to vertical position until the vertical position has changed significantly. This supports the hypothesis of the existence of an optical midplane.

An overlay of representative midplane signals from Figures 12 and 13 which is given in Figure 14 shows that the edge of the arc emission may be seriously affected by the arc refraction. Note however that the refraction patterns in Figure 12 are for the backlight whose rays must traverse the whole chamber. The rays from the arc emission in Figure 13 would not be so strongly affected because those rays need pass the outer refraction zone only once.

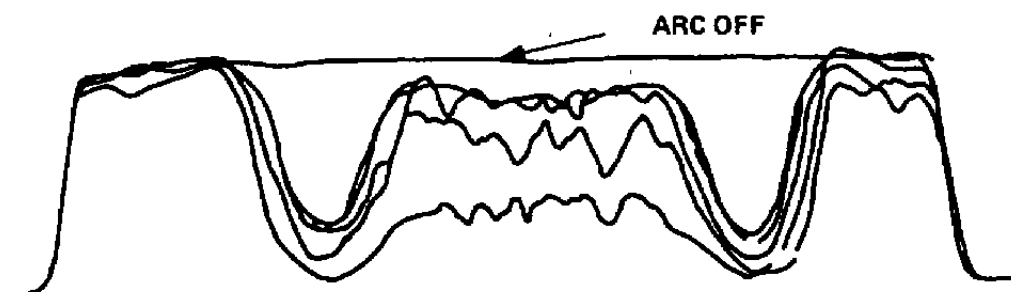


Figure 12. Horizontal Scan at Different Vertical Positions, Backlight Only. $\lambda = 842.35$ nm, Argon Arc, 30 Atm., ~ 15 amp.



Figure 13. Horizontal Scan at Different Vertical Positions. Arc Only. $\lambda = 842.35$ nm, Argon Arc, 30 Atm., ~ 15 amp.

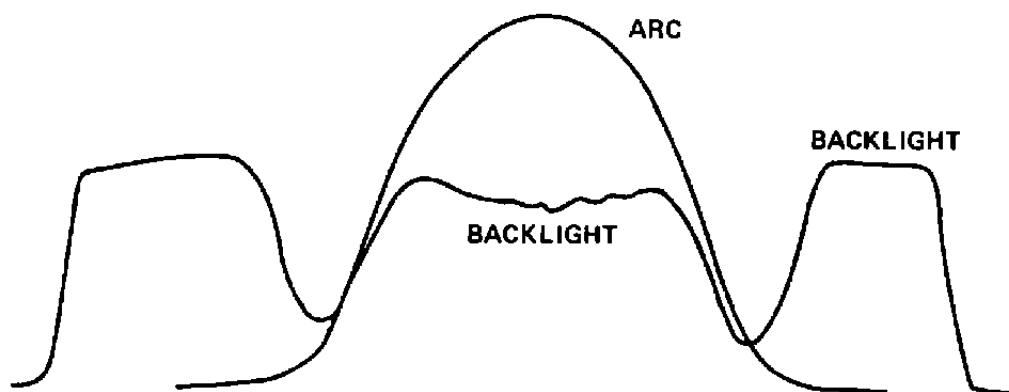


Figure 14. Midplane Scans From Figures 12 and 13 Superimposed.
Vertical Scales Differ.

A midplane scan from Figure 12 is repeated in the middle of Figure 15. The upper figure gives the cascade plate construction from an arc side-view, the lower figure gives the plate construction from the axial view. All sketches are to scale and symmetric about the sketch symmetry lines. The dips in the transmission signal are seen to occur over the copper which lies between the arc channel and the water channels. This is to be expected because the ray shown at lower left passes through a region of strong gradients which are perpendicular to the ray. The path length over which such conditions exist is also the longest in that region of the apparatus.

LASER BACKLIGHT

An He-Ne 2 mwatt laser operating at 632.8 nm, was used as a backlight in all the preliminary laser experiments. In the first experiments, the beam diameter at the arc axis was nearly the same as the visible arc diameter, about 2.5 mm, whereas the window gap was about 1.2 mm. It was obvious for the first time that the vertical gradients in the refractive index caused a very serious problem in these experiments and that much smaller laser beams would be needed. However, information could be obtained on the horizontal ray-bending.

A pin hole placed close to the pressure vessel caused the laser beam to have a diameter of about 0.5 mm. as it passed through the arc. The horizontal plane of the layout is shown in Figure 16. The laser source was diffracted circularly so that the laser spot was 7 mm. in diameter at the opaque screen containing the pin hole. The pin hole was moved laterally by a precision micrometer. In the absence of the lens, at 1 atm., the lateral position, y_i , of the spot on the screen was about twice the position $y_{p.h.}$ of the pin hole, as shown in the lowest data in Figure 17.

The 1 atm. data in Figure 17 is the same with the arc off or on. As the arc pressure is increased to 6.8 atm. and then to 30 atm., refraction occurs. The refraction is greater for larger pressures and for larger off-axis positions of the laser transversal (i.e. greater $y_{p.h.}$).

With the lens in place, focussing the arc axis on the screen, the data for the three pressures falls nearly on the same (dashed) line as the data when the arc is off. This would be rigorously true for an ideal lens if the ray displacement were small and occurred only near the object plane. A possible source of the scatter around the dashed line is the relatively large size of the laser spot and the difficulty of assessing the central ray in the spot.

The refraction angle may be estimated by assuming that the refraction occurred in the central arc plane which is parallel to the screen and that the 1 atm. data represents the unrefracted ray. With the pin hole located at $y_{p.h.} = 1$ mm., so that the ray passes near the luminous edge of the arc, the estimated angles of refraction are:

<u>Pressure</u>		<u>Angle of Refraction</u>
6.8 atm.		.09°
30.0 atm.		.53°
4.4	ratios	5.4

The simple refraction theory given later estimates the angle at 30 atm. to be .15° for a single pass through a circular refractive field for a ray starting within the arc at the central plane at a position 1 mm. off arc axis. For a ray starting outside the arc, the estimated angle of deviation would be about 0.3°. Thus the present experiment (.53°) agrees with the simple theory (.3°) within a factor of 2.

The simple theory asserts that the angle of deviation is proportional to the arc pressure, given identical isotherm patterns. Thus the agreement between the pressure ratio and the angle ratio is reasonable for these preliminary experiments.

As before the vertical refraction of the laser beam became serious as the pressure was increased to 30 atm. Also, between 30 and 50 atm. the emerging laser beam had an unacceptable amount of wandering, presumably due to variations in the gaseous medium between the arc and the pressure vessel window.

To investigate the refraction more carefully, and to reduce the wandering, the optical path was modified.

APPARATUS MODIFICATION II

In the previous apparatus there was about 10 cm. of hot gas between the cascade plates and the outer windows of the pressure vessel. This region of gaseous convection was eliminated by bringing the windows close to the cascade by tubular steel extensions. Between the arc and the windows which sustain the pressure drop is another controlled environment within a tube which Figures 18 and 19 show brings a sapphire window as close to the arc as is physically possible without cutting into the water channels. Seals were again placed around the snouts and the arc region so that the only gas flow would be axial.

Figure 19 shows a mask behind the window on the left. Figure 20 shows the end view of that tube. The metal mask has three 1/4 mm. diameter holes placed on 1 mm. centers and located in the midplane of the window gap. The mask is to be illuminated by the laser from the left in Figure 19 to provide close-in tiny laser sources whose beams pass through a gaseous region only between the windows shown in Figure 19. The central beam passes through the arc center, the others through the arc edge at a radius of 1 mm.

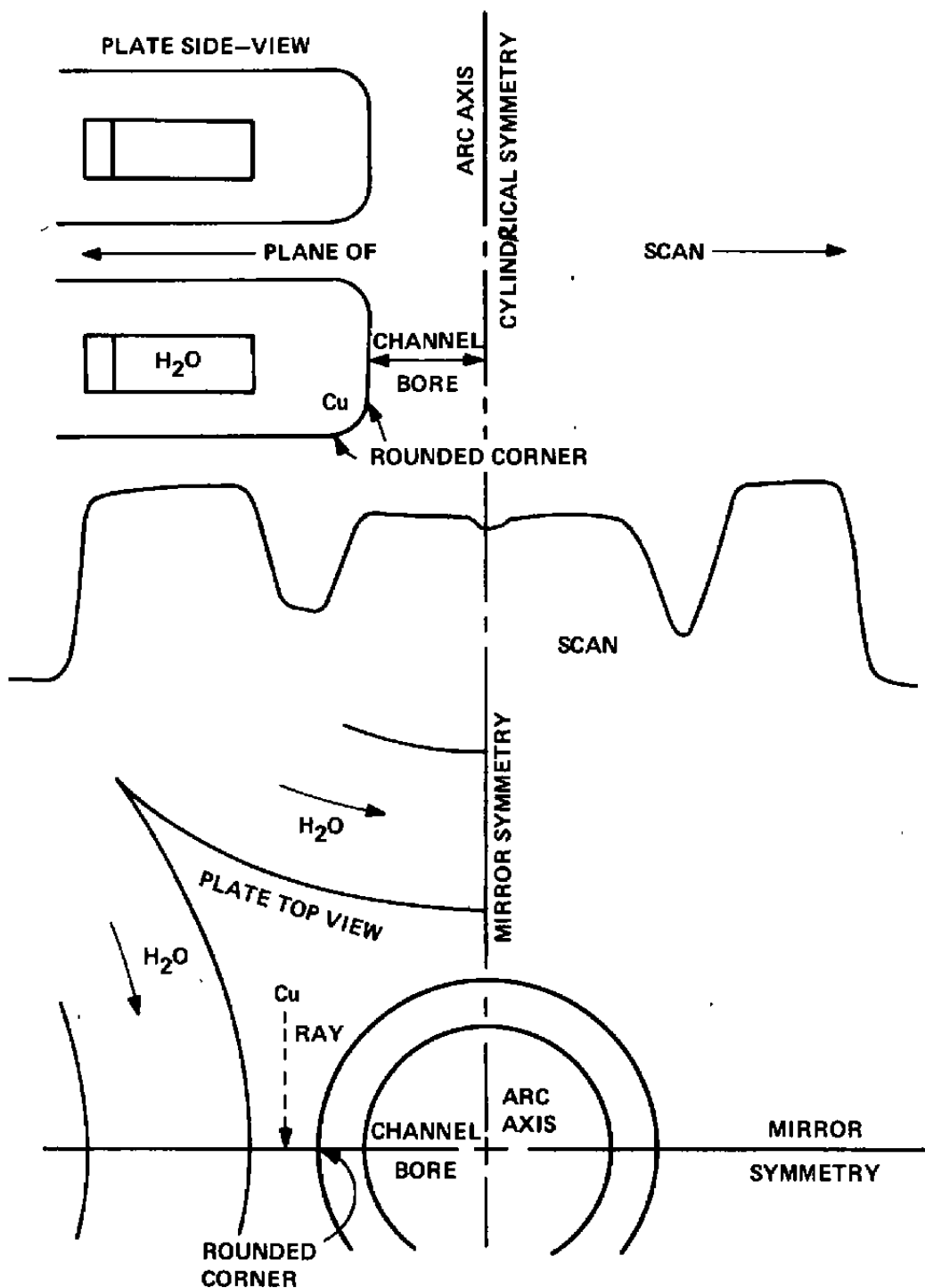


Figure 15. Scaled Relationships of the Scan in Figure 12 to the Apparatus.

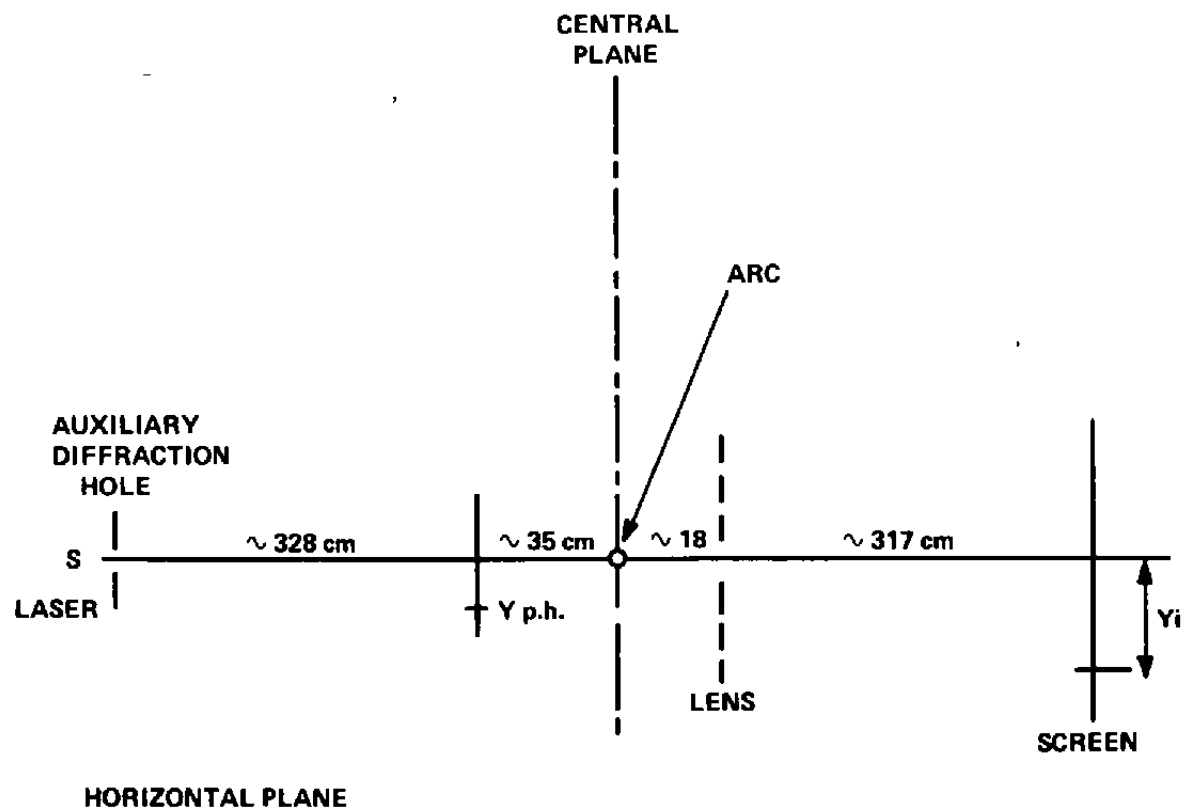


Figure 16. Layout of Preliminary Beam Refraction Experiment.

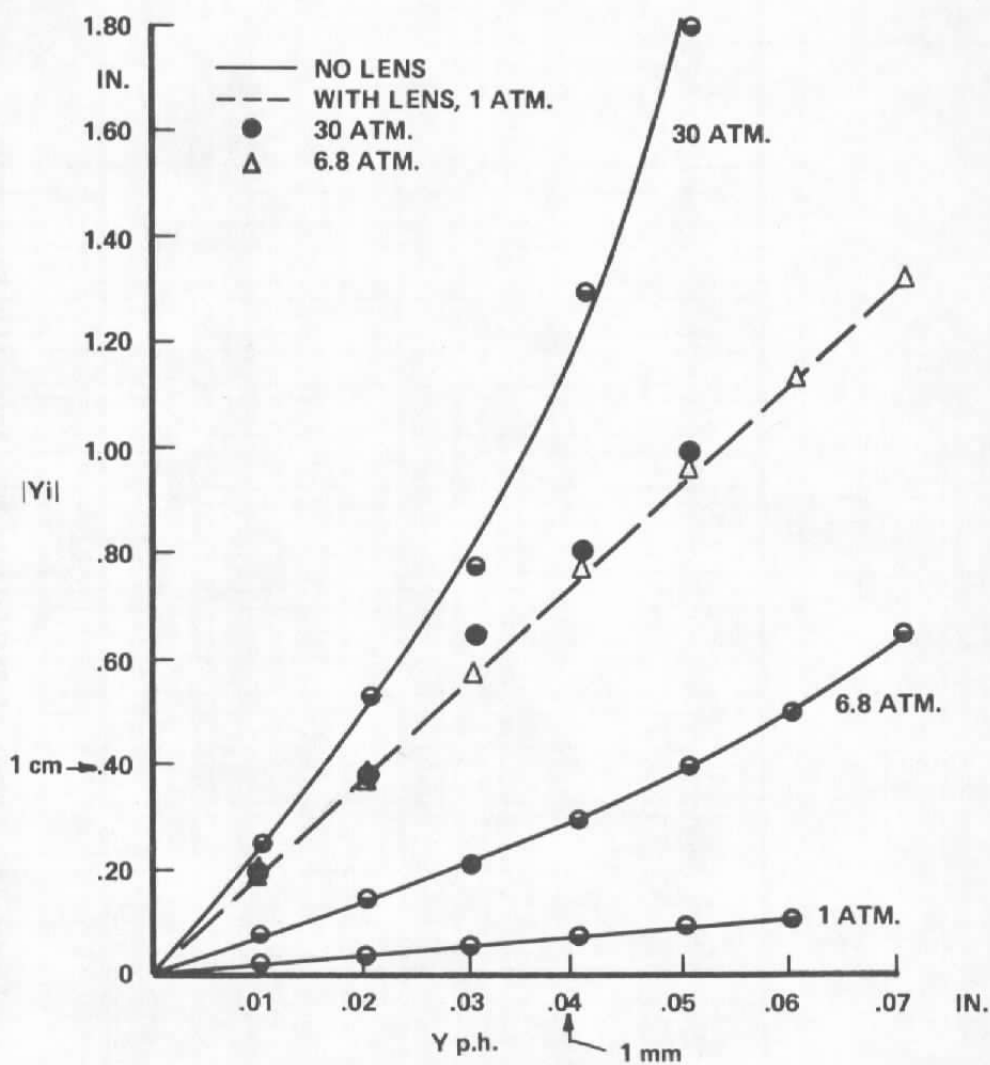


Figure 17. Results of Preliminary Beam Refraction Experiment.

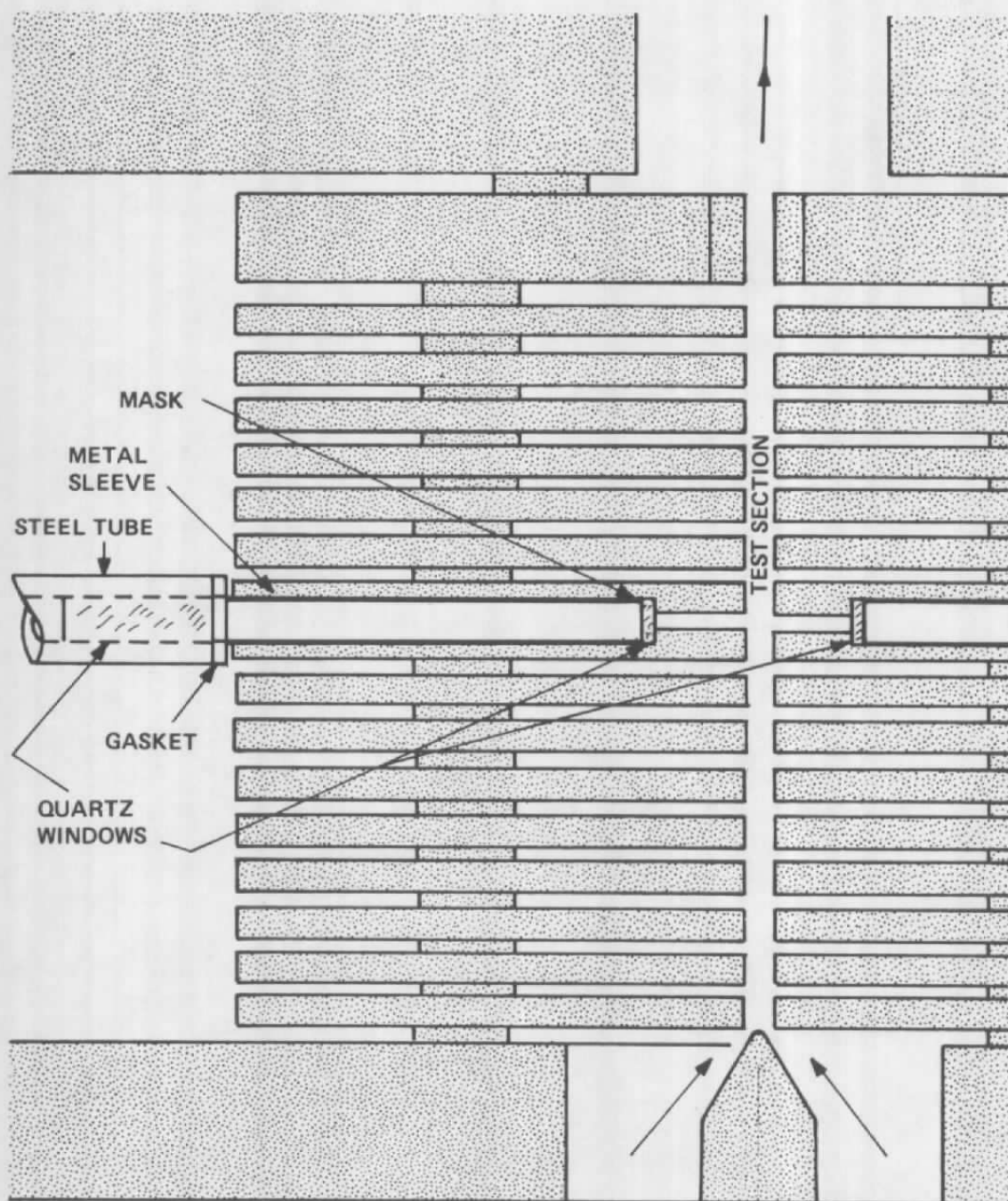


Figure 18. Apparatus Modification, II

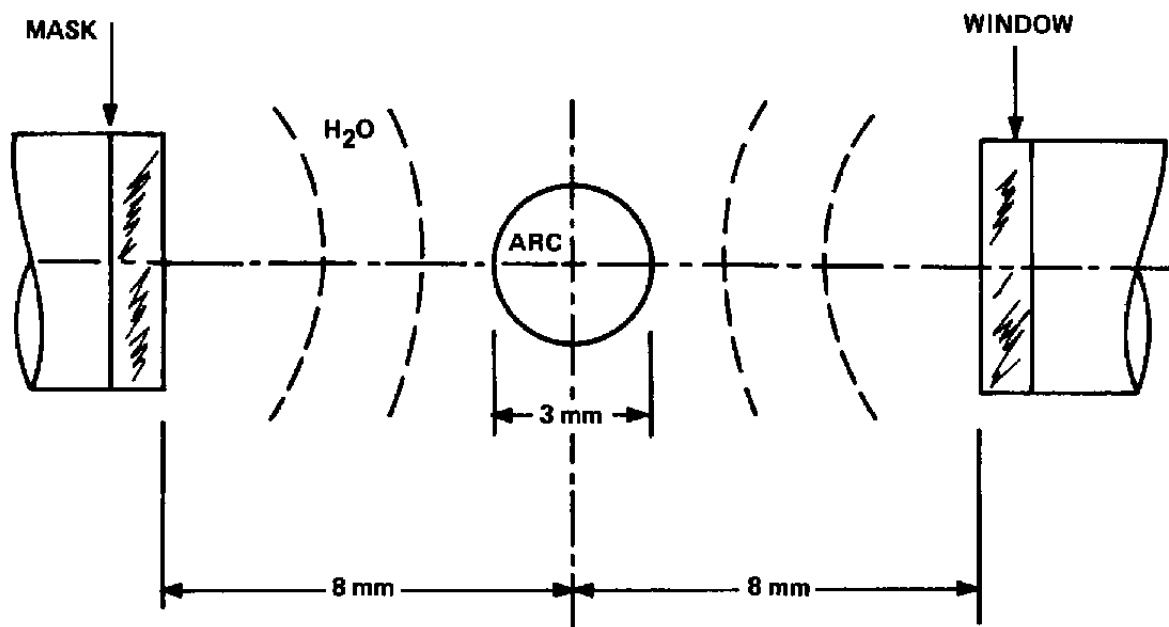


Figure 19. Window Detail of Figure 18.
Top View

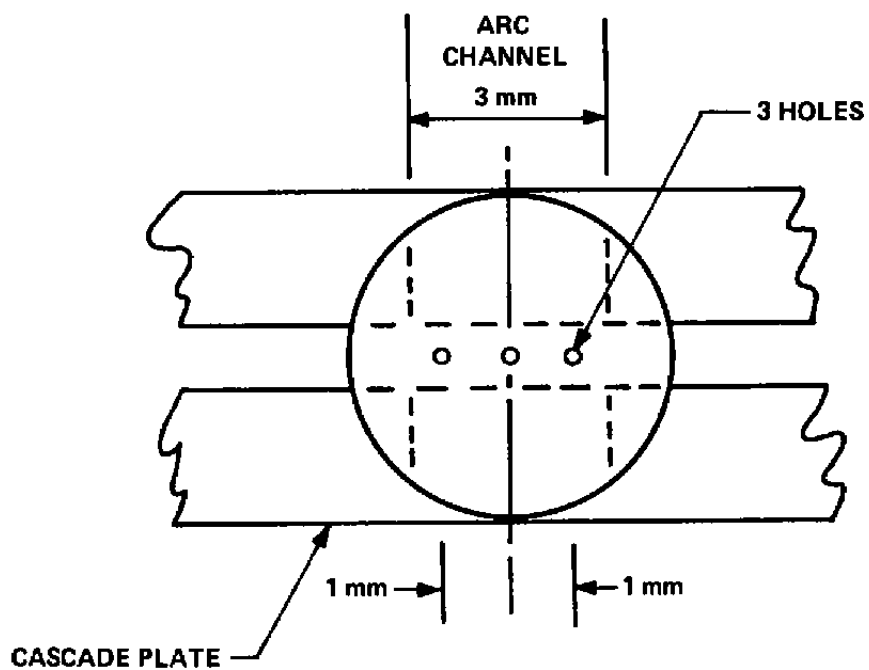


Figure 20. Mask Detail of Figure 19.
End View

ARGON ARC EXPERIMENTS ON REFRACTION, II

The controlled optical path eliminated the wandering in the emerging laser beams.

The pin-hole diameters were chosen as small as possible so as to be good probes of the midplane region, but large enough so that circular diffraction would not prevent their separate identification as they emerged from the pressure vessel. The beams were observed there and again on a screen 2 meters from arc center. A lens was available which if placed at the vessel exit would focus the arc center on the screen, and hence nearly focus the pin-holes also.

It was easily established, by tilting and positioning the backlight laser, that the three tiny beams were travelling the midplane of the cascade plates. As the pressure was increased, the outer beams were refracted more and more away from the central beam, and all three beams were refracted vertically (in the axial direction).

At 30 atm. the beams originally at a radial position of 1 mm. had horizontal (midplane) deviation angles of 0.3° in agreement with theoretical estimates and vertical (axial) deviation angles four or five times greater.

It is important to note as will be discussed later that the beams on the screen appeared to be three vertically straight streaks. That is, wherever the vertical refraction occurred, the information about the horizontal refraction was not obscured.

If the pressurization is repeated with the lens in place, then the round dots on the screen become progressively flatter rectangles, but maintain their positions with respect to the arc.

The latter is understood because all refraction occurs relatively close to the object plane. The change of shape is explained in Figure 21. The lens is in the laboratory environment. If a ray in the upper side of a laser beam is refracted upward, the lens will sense that ray to have come from a position closer to the beam center and will send it to such a place in the image on the screen, thus flattening the originally round beam.

THEORETICAL REFRACTION ESTIMATES

According to Weinberg (Ref. 6), an estimate of the magnitude of the angular deviations produced by refraction in a circularly symmetric isotherm pattern may be obtained in a two temperature field. In reference to Figure 22, a chordal ray at an off-axis position h encounters a discontinuity in the refractive index field. The discontinuity pattern is axisymmetric with respect to the arc axis. The normal and the tangent to the discontinuity are shown. The angles of incidence β_h and refraction β_c and the angle of deviation $\gamma = \beta_h - \beta_c$ are shown. The subscripts stand for "hot" and "cold".

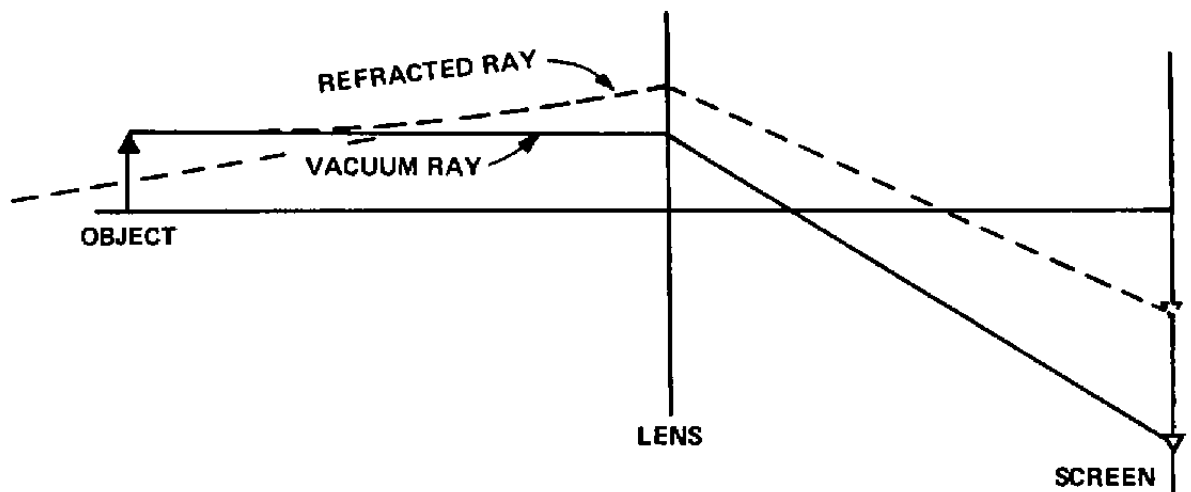


Figure 21. Sketch of Effect of Refraction on Laser Beam Shape.

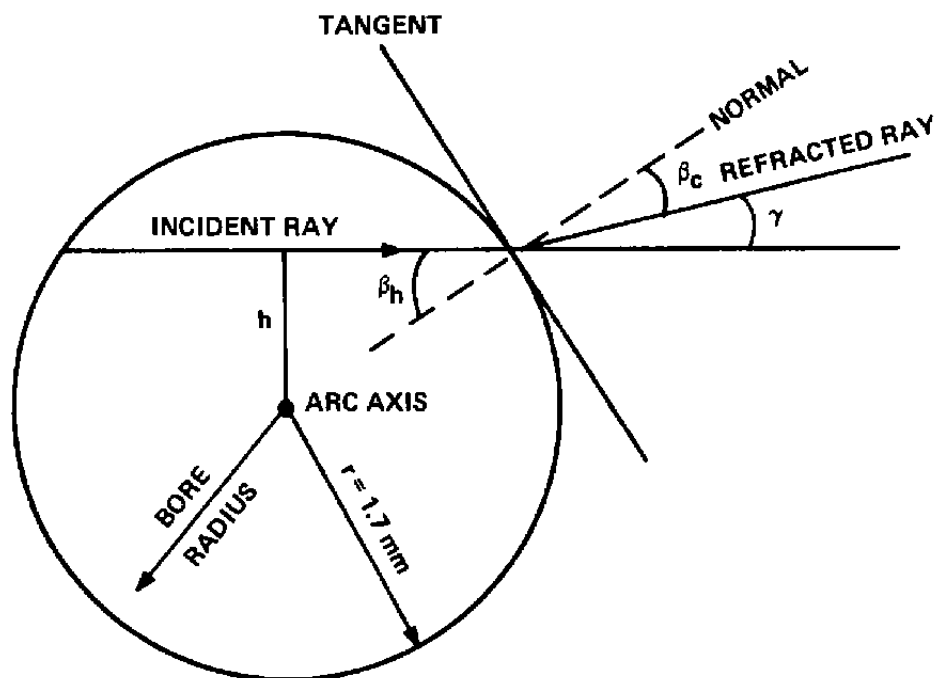


Figure 22. Geometry for Estimating the Angle of Deviation

The index of refraction is taken to be (Ref. 7)

$$n = 1 + \frac{.0733P}{T}$$

where P is in atmospheres and T is in °K. Air or argon can be represented approximately by that formula near N.T.P.

At the boundary, Snell's law applies.

$$\frac{n_c}{n_h} = \frac{\sin \beta_h}{\sin \beta_c}$$

From geometry

$$\sin \beta_c = h/r$$

Typical temperatures were set at

$$T_h = 3000^\circ\text{K} \text{ and } T_c = 500^\circ\text{K} .$$

Solving the above equations for the angle of deviation γ at three pressures of interest, 1, 30, and 100 atm. gives

<u>h</u>	<u>γ_1</u>	<u>γ_{30}</u>	<u>γ_{100}</u>
0 mm.	0 (deg)	0 (deg)	0 (deg)
.2	.0008	.0241	.0794
.4	.0017	.0492	.1620
.6	.0026	.0764	.2516
.8	.0036	.1076	.3540
1.0	.0049	.1458	.4790
1.2	.0066	.1971	.6465
1.4	.0094	.2784	.9102
1.6	.0178	.4684	1.512
1.7	.0322	.8325	2.585

The angular deviations are to be compared with the half-angle of the ray cone from arc center which is accepted by the stops of the present optical system. The half-angle is about 0.7° .

The conclusion is that at some pressure above 1 atm., the ray bending must be accounted for in the deduction of temperature profiles. A more sophisticated approach is needed however, and the optical literature is known to offer different methods. (Ref. 6).

DISCUSSION

This work is part of a larger effort (Ref. 1) in which the arc temperature profiles are needed for the determination of the electrical conductivity and the radiation characteristics are needed in addition for the determination of the thermal conductivity, all properties to be specified as a function of temperature and pressure.

The experiments demonstrate that as the pressure is increased to values near 30 atm. and above, the optical absorption within and outside the air arc column becomes large enough to warrant attention. The same is true for optical refraction for air and argon arcs. The arcs were operated at 12 to 15 amp and were viewed transversely.

Computer programs have been written to take account of the self-absorption and the absorption external to the arc in the deduction of the temperature profiles. In the previous work (Ref. 1), only the OI 844.7 nm. line was used to determine the temperature, and no corrections were made for absorption. Now the work has advanced so that temperature profiles in a 30 atm. air arc are in agreement when deduced from emission and absorption data at the OI 844.7 nm. and the NI 862.9 nm. wavelengths. The agreement may be fortuitous or contain a systematic error, for the effect of refraction has not been assessed.

The magnitude of the corrections are such that the temperature profiles and the electrical conductivity curves previously reported would be shifted about 200°K higher due to external absorption and an additional 50°K higher due to self-absorption corrections at 30 atm. The corrections would be much less at the other reported (Ref. 1) pressures of 1 atm. and 6 atm. However, at 30 atm., such a shift would bring the experimental electrical

conductivity curves into closer agreement with the existing theory (Ref. 1).

A study of the line broadening characteristics of the two lines indicates that the amount of self-absorption within the arc would be comparable at 100 atm. and 30 atm. Thus the techniques applied at 30 atm. should also be successful at the higher pressures of interest.

The absorption outside the arc was identified to be due mostly to NO_2 which has a broad absorption spectrum peaked near 400 nm. Before apparatus modification I, in a 30 atm. air arc there was no usable emission spectrum below ~ 600 nm. reaching the detectors. After modification I, the reduction in the NO_2 concentration along the optical path should be sufficient to allow a calibrated air emission spectrum to be obtained to the limit of the detectors. This has not yet been done but will be necessary in the eventual deduction of thermal conductivity.

The data from modification I might be subject to gas flow effects since the inner windows were omitted. This was checked. For a given air input, the emission and transmission data did reach steady state levels, but did change somewhat if the input was increased. This effect was not pursued for a reading was needed on the refraction problem. Gas flow effects were never observed in the original apparatus (Ref. 1) which did have the inner windows mounted. (See Figure 2).

Apparatus modification II is again sealed against any flow except axial flow and brings the inner windows much closer to the arc than before for the purpose of controlling as much of the optical path as possible. The optical qualities of quartz are still good at 1000°C . Initial experience with this design is good since the windows did not deteriorate physically, and the wandering of a transmitted laser beam at pressures from 30 atm. up to 50 atm. (highest pressure checked) was eliminated.

A mask located on one of the windows allowed three tiny laser beams to be used for the investigation of refraction in an argon arc. The refractive fields within the arc cause the arc to act as a cylindrical diverging lens, and the fields over the water channels appear to act as a stronger orthogonal cylindrical diverging lens. The tiny laser beams which emerge from the mask in Figure 18, traverse the arc, and land on a screen 2 meters away, appear as vertically straight streaks. The straightness of the streaks implies that the information to be gained from the refraction within the arc (horizontal refraction) is not obscured by the refraction over the water channel (vertical refraction).

The angle of deviation increased with pressure, reaching $\sim 1.5^\circ$ vertically at 30 atm., and $\sim 0.3^\circ$ horizontally for a beam traversing the arc near its luminous edge. A lens placed to focus the arc axis on the screen was able to compensate for that amount of deviation.

However, techniques which rely on intensity measurements to determine temperature profiles must clearly account for changes in the shape of the focussed bundles of rays.

Beam mapping methods (Ref. 6) which measure deviation angles as a function of the position of the incoming laser beam would seem to be promising techniques since the vertical refraction has been observed to not obscure the desired knowledge of the horizontal deviation angle due to the arc. However beam mapping techniques depend upon knowledge of the general shape of the isotherms. In a circular pattern, for example, the angle of deviation can be measured as a function of the chordal position of the incoming ray. From that information one can unfold the radial profile of the index of refraction. Given the temperature dependence of the latter, one can then unfold the temperature profile.

CONCLUSIONS

With regard to further refinement of the data at 30 atm. or to extending the original work (Ref. 1) to higher pressures it is clear that a careful quantitative treatment of the effect of refraction in the deduction of the temperature profiles is needed. Work related to this problem has been appearing lately in the scientific literature (Refs. 8,9).

Other parts of the problem seem to be in hand. The apparatus runs well up to the highest pressures tested (143 atm.), the techniques for treating the absorption problems have been established and checked, there are still usable spectral lines at the higher pressures, and the calibrated emission spectrum should be obtainable since the NO_2 concentration has been reduced.

REFERENCES

1. A. V. Larson and J. R. Williams, "Electrical and Thermal Conductivity and Radiation Power of Air Measured at 1-30 Atm. and 6500-11,500°K", Georgia Institute of Technology, Atlanta, Georgia, available as report AEDC-TR-77-69, Arnold Engineering Development Center, June 1977.
2. Daniel P. Dodson, "Preliminary Investigation of Radiation Phenomena in High Pressure Air and Argon Cascade Arcs", M.S. Thesis, Georgia Institute of Technology, December, 1977.
3. J. T. Salmon, Jr., "Radiation Absorption Correction in the Measurement of Temperature in a 30 Atmosphere Air Arc", M.S. Thesis, Georgia Institute of Technology, March, 1978.
4. Hans R. Griem, Plasma Spectroscopy, McGraw-Hill, New York, 1964.
5. F. Cabannes and J. Chappelle, "Spectroscopic Plasma Diagnostics," Reactions Under Plasma Conditions, ed. M. Venugopalan, Vol. 1, Wiley-Interscience, New York, 1971.
6. Felix J. Weinberg, Optics of Flames, Butterworths, Washington, 1963.
7. Handbook of Chemistry and Physics, 56th Edition, 1975-1976, CRC Press.
8. V. Oklobdzua and N. Konjevic, J. Quant. Spectrosc. Radiat. Transfer, 14, 389 (1974).
9. S. Popvic and N. Konjevic, J. Quant. Spectrosc. Radiat. Transfer, 16, 15 (1976).